



Bruce H. Morimoto

# Davunetide

## Pharmacokinetics and distribution to brain after intravenous or intranasal administration to rat

BRUCE H. MORIMOTO<sup>1\*</sup>, INÉS DE LANNOY<sup>2</sup>, ANTHONY W. FOX<sup>1</sup>, ILLANA GOZES<sup>1</sup>, ALISTAIR STEWART<sup>1</sup>

\*Corresponding author

1. Allon Therapeutics Inc., 506-1168 Hamilton Street, Vancouver, BC V6B 2S2, Canada

2. NoAb BioDiscoveries Inc., 8-2820 Argentia Road, Mississauga, ON L5N 8G4, Canada

**ABSTRACT** *Davunetide or NAPVSIQ is a neuroactive peptide which stabilizes microtubules and is currently in clinical development for neurodegenerative diseases like Alzheimer's and frontotemporal dementia. As with most peptide drugs, selection of the route of administration is important and understanding the pharmacokinetics and tissue distribution provides valuable information about the mechanism by which the peptide reaches the central nervous system (CNS). The intranasal bioavailability of davunetide in rat plasma appears to be dependent on the residence time in the nasal cavity, since intranasal administration in anesthetized rats resulted in ~100 percent bioavailability. After either intranasal or intravenous administration, davunetide rapidly appeared in the cerebrospinal fluid (CSF). These results combined with timed tissue distribution data, indicate the mechanism by which intranasal davunetide gets to the CNS is via the systemic circulation and not by direct nose-to-brain transport.*

### INTRODUCTION

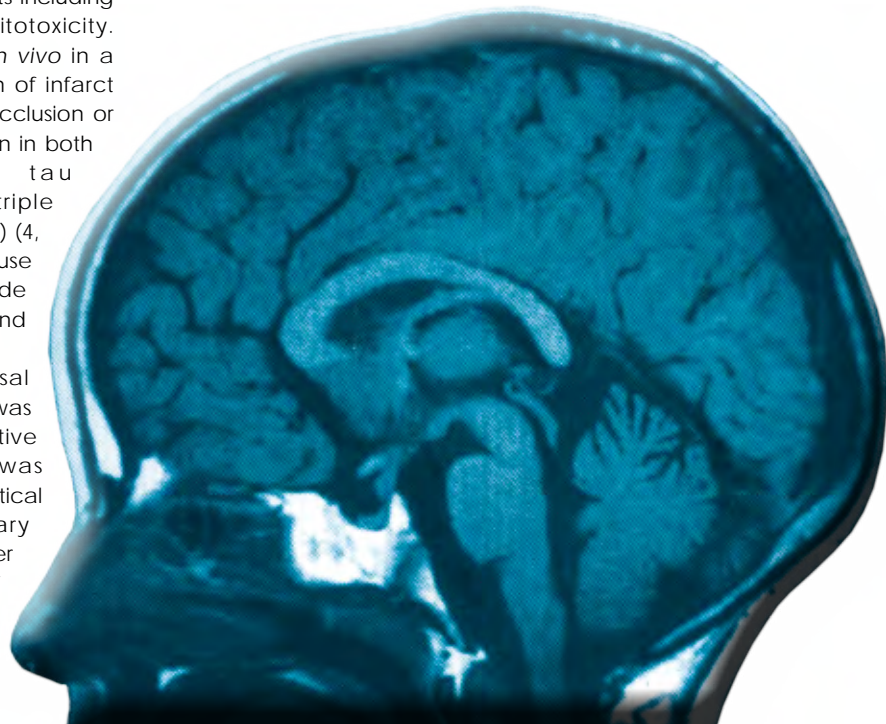
Davunetide, an eight amino acid peptide (also known as NAPVSIQ or NAP peptide), derived from activity-dependent neuroprotective protein, facilitates neuroprotection and improves cognitive performance as supported by a number of preclinical studies (1). Neuroprotection by davunetide is conferred *in vitro* to a variety of insults including oxidative stress, beta amyloid toxicity and excitotoxicity. Neuroprotection has also been demonstrated *in vivo* in a number of models of disease including reduction of infarct volume after permanent middle cerebral artery occlusion or closed-head injury (2, 3). More recently, a reduction in both amyloid peptide accumulation and tau hyperphosphorylation was observed in the triple transgenic mouse model of Alzheimer's disease (AD) (4, 5) as well as in the apolipoprotein E-deficient mouse model (6). Further experiments identified davunetide as neurotrophic, stimulating neurite elongation and synapse formation (7).

In a phase 2 clinical trial, twice daily intranasal administration of davunetide (known as AL-108) was safe and well-tolerated in amnesic mild cognitive impaired patients. Significant improvement was observed in 2 measures of memory, although statistical significance was not observed on the primary endpoint or secondary endpoints evaluating other cognitive domains. Overall, the incidence of

adverse events was similar between placebo- and davunetide-treated groups. Headache and nasopharyngeal events were reported more frequently by davunetide-treated subjects.

Cumulative evidence suggests that neurodegenerative diseases and psychiatric illnesses are associated with cytoskeletal alterations in neurons which result in loss of synaptic connectivity and a compromised ability to transmit axonal information (8-10). As such, neuronal cytoskeleton can be a target for drug therapy, and disturbances in the cytoskeletal architecture and micro-tubule function have been associated with poor cognitive performance in animal models (11). Furthermore, microtubule-dependent transport is impaired in AD (12) and axonopathies have been reported in different AD animal models, suggesting that perturbed microtubule transport may underlie cognitive deficits observed in AD (10, 13, 14).

Davunetide facilitates neuroprotection and improves cognitive performance as supported by numerous *in vitro* and *in vivo* preclinical studies (15). The proposed mechanism of action of davunetide is maintenance and stabilization of the micro tubular network (15, 16). The objective of this study is to evaluate the plasma and CSF pharmacokinetics and tissue distribution of davunetide following intravenous and intranasal administration. Preliminary pharmacokinetic data for davunetide was previously presented (17). Brain bioavailability and the mechanism by which intranasal davunetide penetrates the CNS is presented.



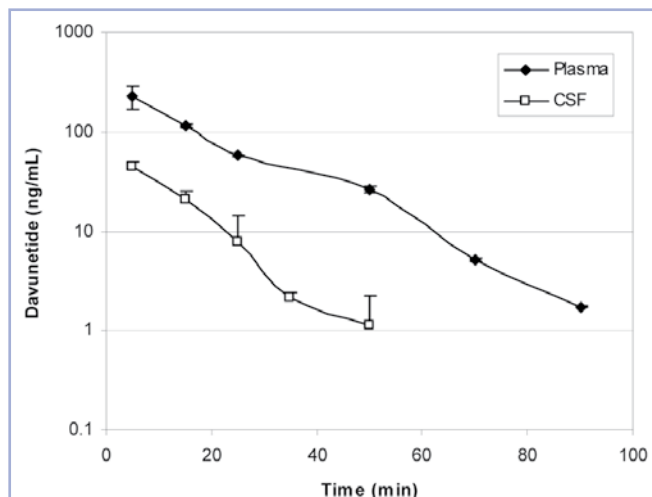


Figure 1. Concentration of Davunetide in Plasma and CSF after Intravenous Administration. Mean ( $\pm$  S.D.) davunetide concentrations in serial plasma and CSF samples following intravenous bolus administration of 12.5 mg to 3 rats.

Parameter	Units	Intravenous (n=3)	Intranasal (n=5)
Dose	mg	12.5 $\pm$ 0.854	10.3 $\pm$ 0.110
$t_{max}$	min	5.00 $\pm$ 0.000	19.0 $\pm$ 8.94
$C_{max}$	ng/mL	229 $\pm$ 61.7	131 $\pm$ 70.3
Terminal half-life	min	12.2 $\pm$ 0.208	70.7 $\pm$ 34.0
$AUC_{0-inf}$	min*ng/mL	4611 $\pm$ 395	5279 $\pm$ 2669
$MRT_{inf}$	min	20.1 $\pm$ 1.72	75.5 $\pm$ 19.1
CL	L/min/kg	8.99 $\pm$ 0.757	n/a
$V_{ss}$	L/kg	182 $\pm$ 31.2	n/a
F	%	100	101 $\pm$ 49.9

n/a denotes not applicable.

Table 1. Estimated pharmacokinetic parameters for davunetide in plasma following intravenous and intranasal administration of davunetide to rats (data represent the mean  $\pm$  S.D.).

## MATERIALS AND METHODS

Davunetide (Lot number FN8Q0201A) was manufactured by fmoc-solid phase synthesis, HPLC purified, converted to the acetate salt and lyophilized (Bachem California). The peptide purity was 99 percent.  $^{14}C$ -Davunetide was synthesized by hybrid solid-solution phase (MDS Pharma Services, Montreal, Canada). Briefly, solid phase synthesis was used to create the protected and resin-bound 6 amino acid peptide, PVSIPQ.  $^{14}C$ -Alanine was incorporated into the asparagine-alanine dipeptide and coupled to the hexapeptide in solution phase. Following HPLC purification, the specific activity of  $^{14}C$ -davunetide was 42.2 mCi/mg with 98.6 percent purity (Lot number FD-MDSPSRS-VII-268).

### Pharmacokinetics

Male Sprague-Dawley rats (Charles River Labs, St. Constant, QC, Canada) weighing 290 to 323 g were implanted with catheters in the femoral artery (for serial blood collection) and femoral vein (for intravenous administration and blood sample volume replacement) and a cannula in the cisterna magna (for serial CSF collection). For intravenous (*i.v.*) administration, davunetide was dissolved in sterile 0.9 percent sodium chloride for injection at a concentration of 15 mg/mL. For intranasal (*i.n.*) administration, davunetide was dissolved at a concentration of 250 mg/mL in 7.5 mg/mL sodium chloride, 1.7 mg/mL citric acid monohydrate, 3.0 mg/mL disodium phosphate dihydrate, and 0.2 mg/mL 50 percent (w/w)

benzalkonium chloride, pH 5.1. Davunetide was administered at a dose of 30 mg/kg (2 mL/kg) intravenously (n=3) or 10 mg/animal (20  $\mu$ L per nostril, 28-33 mg/kg) intranasally (n=5) to anesthetized rats. Serial CSF samples were collected at a rate of 2  $\mu$ L/min over 10 to 60 min intervals from each animal. Serial plasma samples were collected at pre-dose, 5, 15, 25, 35, 50, 70, 90, 110, 135, 165 and 210 minutes (*i.v.*) or pre-dose, 5, 15, 25, 35, 45, 55, 70, 90, 110, 135, and 165 min (*i.n.*), representing the midpoint of each CSF collection interval. Validated bioanalytical methods were used for quantification of davunetide in plasma, CSF and dosing solution samples. Sample analysis was conducted using a PE Sciex API 4000 MS/MS system equipped with an Agilent 1100 HPLC. The method was linear over the range of 0.750 – 150 ng/mL davunetide. Data was analyzed by non-compartmental methods using WinNonlin Pro 4.0 (Pharsight Corp., Mountain View, CA).

### Whole body autoradiography

A total of 30 Sprague-Dawley rats were given formulated  $^{14}C$ -davunetide (specific activity: 41 mCi/g) at a target dose of 20  $\mu$ Ci/animal and 30 mg/kg by intranasal administration (Group 1, 15 animals, 20  $\mu$ L/naris, actual dose 17.9 mg/kg) or intravenous (Group 2, 15 animals, 2 mL/kg, actual dose 28.8 mg/kg). Blood samples were collected from treated animals at the time-points described below. Radioactivity in whole blood and plasma samples was measured by liquid scintillation counting. Following sacrifice, radioactivity in tissues was obtained by quantitative whole-body autoradioluminography (QWBA). The metabolite profile

in plasma was assessed by HPLC with radiochemical detection.

Blood and plasma were collected from three animals at 5, 15, 30, 60 and 240 minutes post-dose. The metabolite profile in plasma was determined by HPLC radiometric and mass spectroscopic detection. Immediately following euthanasia, animals were frozen and embedded for sagittal whole-body sections. Sections were then freeze-dried and autoradioluminograms made. Radioactivity associated with a given tissue was quantified and corrected for background.

## RESULTS

### Intravenous administration

Following *i.v.* administration, davunetide appeared in both plasma and CSF (Figure 1). The CSF  $C_{max}$  was 45.1  $\pm$  4.88 ng/mL measured during the first 10 min collection interval. The terminal elimination half-lives of davunetide in plasma and CSF were estimated as 12.2  $\pm$  0.208 min and 9.34  $\pm$  4.00 min ( $K_{elim} = 3.41$  and 4.45  $h^{-1}$ ), respectively (Tables 1 and 2). The estimated total body clearance (CL) of davunetide was 2715  $\pm$  258 mL/min and this corresponded to the short elimination half-life in plasma. The estimated steady-state volume of distribution ( $V_{ss}$ ) was 54.9  $\pm$  9.16 L, i.e., larger than the total body water at  $\geq$  250 L/kg). The ratio of the area under the concentration versus time curve for CSF to that for plasma (in the absence of a correction for unbound fraction

in plasma) was less than unity ( $0.138 \pm 0.0159$ ). A plot of the plasma concentration versus CSF concentration results in a linear correlation (Figure 2).

#### Intranasal administration

Following intranasal administration, davunetide appeared rapidly in plasma ( $T_{max} = 19.0 \pm 8.94$  min) with a  $C_{max}$  of  $131 \pm 70.3$  ng/mL (Figure 3). The estimated terminal elimination half-life of davunetide in plasma was  $70.7 \pm 34.0$  min and the mean residence time was  $75.5 \pm 19.1$  min, significantly greater than that following *i.v.* administration

Parameter	Units	Intravenous (n=3)	Intranasal (n=5)
$t_{max}$	min	$5.00 \pm 0.00$	$11.0 \pm 8.94$
$C_{max}$	ng/mL	$45.1 \pm 4.88$	$3.48 \pm 0.718$
Terminal half-life	min	$9.34 \pm 4.00$	nc
$AUC_{0-inf}$	min*ng/mL	$641 \pm 123$	nc
$MRT_{inf}$	min	$14.8 \pm 1.69$	nc
CSF/Plasma $AUC_{0-inf}$ Ratio		$0.138 \pm 0.0159$	nc

nc denotes not calculable due to insufficient data during terminal phase.

Table 2. Estimated pharmacokinetic parameters for davunetide in CSF following intravenous and intranasal administration of davunetide to rats (data represent the mean  $\pm$  S.D.).

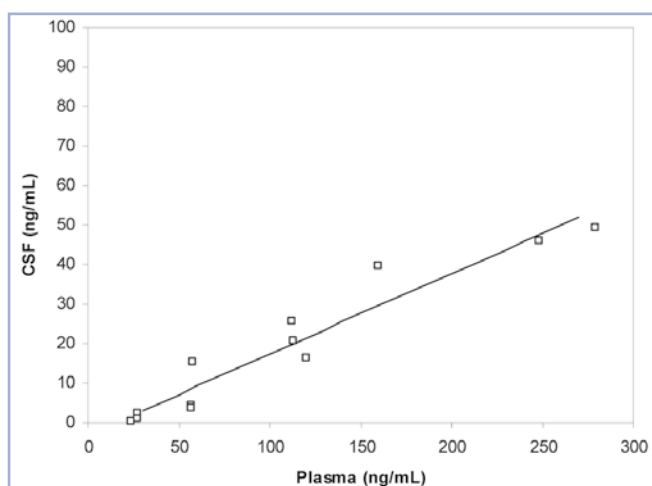


Figure 2. Correlation of Davunetide Plasma and CSF Concentrations After Intravenous Administration. Linear regression analysis of CSF versus plasma concentrations of davunetide following intravenous bolus administration of 12.5 mg davunetide to 3 rats.

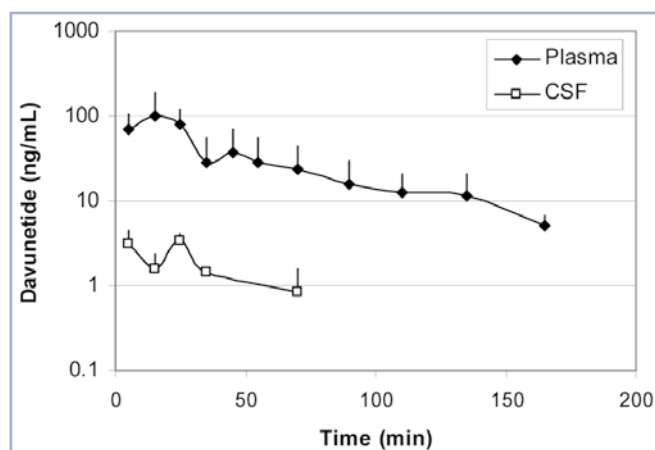


Figure 3. Concentration of Davunetide in Plasma and CSF after Intranasal Administration. Mean ( $\pm$  S.D.) davunetide concentrations in serial plasma and CSF samples following intranasal administration of 10 mg of davunetide to 5 rats.

(Table 1). The intranasal dose was completely bio available ( $F^{in} = 101 \pm 49.9$  percent) when compared to the *i.v.* data (Figure 1 and Table 1). As the rats were anesthetized, the intranasal cavity may have acted as a reservoir for the dosing solution and as a result a steady absorption of davunetide over time from the nasal cavity occurred.

Davunetide also appeared relatively rapidly in the CSF with a  $C_{max}$  of  $3.48 \pm 0.718$  ng/mL measured during the first three 10 min collection intervals ( $T_{max} = 20-30$  min). The terminal elimination half-life could not be calculated for CSF due to the low CSF concentrations which declined rapidly below the lower level of quantitation (0.750 ng/mL).

#### Tissue distribution

A whole body autoradiography study was conducted to evaluate the tissue distribution of radioactive davunetide after either intravenous or intranasal administration. The plasma and blood radioactivity concentration values were significantly higher for intravenous administration than for intranasal (intranasal: 0.1-3.7  $\mu$ g eq/mL, intravenous: 5.2-54.5

$\mu$ g. eq/mL). Blood content values were 7.7 percent after intravenous administration at 5 minutes post-dose, but after intranasal administration these were below 1.2 percent for all time-points. The blood to plasma ratios were relatively constant, ranging between 0.65 - 0.81 for both intranasal and intravenous dose groups over the study interval. The radioactivity in plasma was assessed to be intact peptide by HPLC with radiometric detection. The radioactive concentration in plasma after *i.v.* or *i.n.* administration is presented in Figure 4.

After intranasal administration, the highest tissue radioactivity concentration and AUC were obtained from the nasal turbinates (at 5 minutes post-dose). High radioactivity levels were also observed in the lumens of the stomach and small intestine, consistent with conscious animals swallowing of part of the dose administered. Distribution of radioactive davunetide was observed in the adipose tissue (white fat), brain, cisterna magna (marker for CSF), eye, seminal vesicle

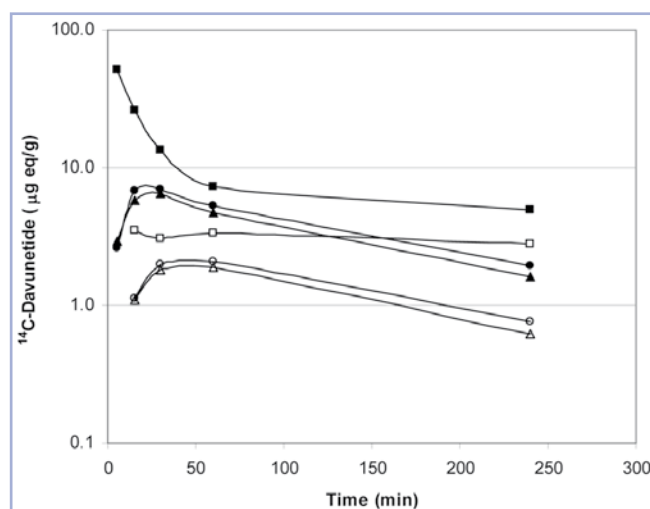


Figure 4. Distribution of  $^{14}C$ -Davunetide. Radioactive distribution of davunetide in plasma (squares) and to the brain (triangles) or olfactory bulb (circles) after intranasal (open symbols) or intravenous (closed symbols) administration.

and testis; mean radioactivity concentrations were low. The olfactory bulb and spinal cord also had low radioactivity levels.

After intravenous administration, the radioactivity levels in tissues were generally high. The highest tissue radioactivity and AUC values were obtained from the kidney, Harderian gland and pancreas. The distribution of davunetide in other tissues was similar to intranasal administration.

Intravenous administration resulted in higher tissue radioactivity levels than after intranasal administration. This is likely due, at least in part, to ~1.6 times more radioactivity administered to the intravenous animals (28.8 mg/kg compared to 17.8 mg/kg), but also due to the dose route. Tissue to plasma ratios increased during the study interval suggesting that radioactivity was cleared faster from plasma than from tissues.

To directly compare tissue concentrations and exposure after intranasal or intravenous administration, the radioactive concentrations measured in the brain, olfactory bulb and cisterna magna were normalized for dose (radioactive concentration divided by the dose). The results of this transformation are presented in Table 3. Despite the difference in the amount of radioactivity administered, uniformly greater radioactive exposure was observed after intravenous administration (Figure 4).

## DISCUSSION

The pharmacokinetics of davunetide suggests that the bioavailability after *i.n.* administration depends on the residence time in the nasal cavity. The apparent terminal elimination half-life is longer after *i.n.* administration compared to *i.v.* (70 min versus 12 min). This is consistent with the hypothesis that sustained absorption occurred in the anesthetised rat, which not only results in a longer apparent half-life but also gives rise to ~100 percent bioavailability. Collectively, these results indicate permeability is not limiting for davunetide and increasing the residence time in the nasal cavity should improve bioavailability of the intranasal product.

Typically, it is presumed that peripheral routes of administration expose the central nervous system in a manner that is comparable to systemic exposure unless there is sequestration in this tissue or failure to penetrate it. Pharmacokinetic information from intravenous administration (*i.e.*,  $F = 1.0$ , complete absorption) can then usually be used when compared with pharmacokinetic information from the alternative route of administration to delimit the hazard that intranasal administration would cause unanticipated central nervous system exposure.

Frey and colleagues have proposed direct delivery of drugs from the intranasal site of absorption to the central nervous system (18), a proposal which was recently reviewed (19). Although this is an intriguing hypothesis for CNS acting drugs, it does not appear to be the case for davunetide. When davunetide was measured in serial samples of plasma and CSF after an equivalent dose either by intravenous or intranasal administration, CSF exposure was substantially greater after intravenous administration (Figures 1 and 3), despite nearly identical systemic exposure (Table 1). Therefore, preferential distribution to the CSF did not occur after intranasal administration as would be predicted by the direct nose-to-brain hypothesis. Davunetide appeared rapidly in the plasma after intranasal administration, with a  $T_{max}$  of ~20 min (Figure 3). The  $C_{max}$  in CSF appears to lag that of plasma, suggesting that the kinetics of davunetide appearance in plasma precedes

Time (min)	Intranasal			Intravenous		
	Brain	Olfactory bulb	Cisterna magna	Brain	Olfactory bulb	Cisterna magna
5	-	-	-	102	91	202
15	62	63	43	200	233	198
30	101	110	106	224	240	165
60	107	116	33	164	185	89
240	37	43	28	56	68	28

Units: (ng equivalent \* kg) per (gram tissue \* mg dose)

Table 3. Radioactive tissue concentration normalized for dose.

that in the CSF. This implies that intranasal administration results in rapid absorption into the plasma with subsequent transport across the blood-brain-barrier into the CSF (and CNS).

Evidence against a potential direct nose-to-brain path is further supported by data from the radioactive distribution study. In Figure 4, the radioactive concentration in either the brain or olfactory bulb is plotted as a function of time after intranasal or intravenous administration. The distribution into the brain and olfactory bulb are identical and independent of the route of administration. Moreover, radioactivity in the olfactory bulb did not kinetically precede that of the brain, and the ratio of radioactive concentration in the brain-to-olfactory bulb is unity (one) for both intranasal and intravenous administration.

## ACKNOWLEDGEMENTS

We thank the staff of NoAb BioDiscoveries, Charles River Laboratories Montreal, and Allon Therapeutics for their valuable contributions to this study. Illana Gozes serves as a Professor at Tel Aviv University, the Lily and Avraham Gildor Chair for the Investigation of Growth Factors, and Director of the Adams Super Centre for Brain Studies.

## REFERENCES AND NOTES

- I. Gozes, B.H. Morimoto et al., *CNS Drug Reviews*, 11, pp. 363-378 (2005).
- L. Beni-Adani, I. Gozes et al., *J Pharmacol Exp Ther.*, 296, pp. 57-63 (2001).
- R.R. Lecker, A. Teichner et al., *Stroke*, 33, pp. 1085-1092 (2002).
- Y. Matsuoka, A.J. Gray et al., *J Mol Neurosci.*, 31, pp. 165-170 (2007).
- Y. Matsuoka, Y. Jouroukhin et al., *J Pharmacol Exp Ther.*, 325, pp. 146-153 (2008).
- M. Bassan, R. Zamostiano et al., *J Neurochem.*, 72, pp. 1283-1293 (1999).
- V.L. Smith-Swintosky, I. Gozes et al., *J Mol Neurosci.*, 25, pp. 225-238 (2005).
- S.E. Arnold, V.M. Lee et al., *Proc Natl Acad Sci USA*, 88, pp. 10850-10854 (1991).
- G. Benitez-King, G. Ramirez-Rodriguez et al., *Curr Drug Targets CNS Neurol Disord.*, 3, pp. 515-533 (2004).
- G.B. Stokin, C. Lillo et al., *Science*, 307, pp. 1282-1288 (2005).
- E. Chevallier-Larsen, E.L. Holzbaur, *Biochim Biophys Acta*, 1762, pp. 1094-1108 (2006).
- P.W. Baas, L. Qiang, *Trends Cell Biol.*, 15, pp. 183-187 (2005).
- J. Gotz, L.M. Ittner, *J Neurochem.*, 98, pp. 993-1006 (2006).
- S. Kins, K. Beyreuther, *Nat Med.*, 12, pp. 764-765 (2006).
- I. Divinski, L. Mittelman et al., *J Biol Chem.*, 279, pp. 28531-28538 (2004).
- I. Divinski, M. Holtser-Cochav, *J Neurochem.*, 98, pp. 973-984 (2006).
- B.H. Morimoto, A.W. Fox et al., *Drug Metab Rev.*, 38(Suppl 2), pp. 213-214.
- W.H. Frey, *Drug Del Technol.*, 2, pp. 46-49 (2002).
- W.H.M. Merkus, M.P. van den Berg, *Drugs R.D.*, 8, pp. 133-144 (2007). 